Finding Adversarially Robust Graph Lottery Tickets

Anonymous authors
Paper under double-blind review

Abstract

Graph Lottery Tickets (GLTs), comprising a sparse graph neural network (GNN) and a sparse input graph adjacency matrix, can significantly reduce the inference compute footprint compared to their dense counterparts. However, their performance against adversarial attacks remains to be fully explored. In this paper, we first investigate the resilience of GLTs against different structure perturbation attacks and observe that they are vulnerable and show a large drop in classification accuracy. We then present an *adversarially robust graph sparsification (ARGS)* framework that prunes the adjacency matrix and the GNN weights by optimizing a novel loss function capturing the graph homophily property and information associated with both the true labels of the train nodes and the pseudo labels of the test nodes. By iteratively applying ARGS to prune both the perturbed graph adjacency matrix and the GNN model weights, we can find adversarially robust graph lottery tickets that are highly sparse yet achieve competitive performance under different training-time structure attacks. Evaluations conducted on various benchmarks, considering different poisoning structure attacks such as PGD, MetaAttack, PR-BCD, GR-BCD, and adaptive attacks, demonstrate that the GLTs generated by ARGS can significantly improve their robustness, even when subjected to high levels of sparsity.

1 Introduction

Graph neural networks (GNNs) (Hamilton et al., 2017; Kipf & Welling, 2016; Veličković et al., 2017; Zhou et al., 2020; Zhang et al., 2020) achieve state-of-the-art performance on various graph-based tasks like semi-supervised node classification (Kipf & Welling, 2016; Hamilton et al., 2017; Veličković et al., 2017), link prediction (Zhang & Chen, 2018), and graph classification (Ying et al., 2018). The success of GNNs is attributed to the neural message-passing scheme in which each node updates its feature by recursively aggregating and transforming the features of its neighbors. However, the effectiveness of GNNs when scaled up to large and densely connected graphs is impacted due to high training and inference cost and substantial memory consumption. Unified graph sparsification (UGS) (Chen et al., 2021) addresses this concern by simultaneously pruning the input graph adjacency matrix and the GNN to show the existence of a graph lottery ticket (GLT), a pair of sparse graph adjacency matrix and GNN model, which can substantially reduce inference cost without compromising model performance.

Recent studies reveal that GNNs are vulnerable to adversarial attacks (Dai et al., 2018; Wu et al., 2019; Zügner & Günnemann, 2019; Mujkanovic et al., 2022; Jin et al., 2020a). An adversarial attack on the graph structure introduces unnoticeable perturbations by inserting, deleting, or rewiring edges in the graph. These perturbations increase the distribution shift between train and test nodes in the graph, fooling the GNN to misclassify nodes (Li et al., 2023b) in the transductive node classification task. To counter these attacks, many defense techniques have been developed. Some techniques improve the node classification accuracy of GNNs by cleaning the perturbed graph structure (Wu et al., 2019; Entezari et al., 2020; Jin et al., 2020b; Deng et al., 2022; Zhu et al., 2021b); others improve the accuracy by modifying the GNN architecture (Zhang & Zitnik, 2020; Geisler et al., 2021; Zhu et al., 2019). Although GLTs demonstrate strong performance on original benign graph data, their performance in the presence of adversarial structure perturbations remains largely unexplored. Achieving adversarially robust GLTs (ARGLTs) can enable efficient GNN inference under adversarial threats.

We address this challenge by first investigating empirically the resilience of GLTs identified by UGS against different structure perturbation attacks (Zügner & Günnemann, 2019; Liu et al., 2019; Mujkanovic et al., 2022) and showing that they are vulnerable. We then present ARGS (Adversarially Robust Graph Sparsification), an optimization framework that, given an adversarially perturbed graph, iteratively prunes the graph adjacency matrix and the GNN model weights to generate an adversarially robust graph lottery ticket (ARGLT) which achieves competitive node classification accuracy while exhibiting high levels of sparsity.

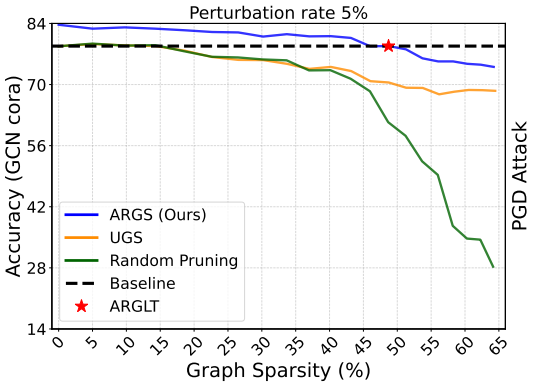

Figure 1: Comparison of different graph sparsification techniques in accuracy vs. graph sparsity. ARGS achieves similar accuracy with 35% more sparsity for the Cora dataset under PGD attack.

Adversarial attacks like the projected gradient descent (PGD) attack (Wu et al., 2019), the meta-learning-based graph attack (MetaAttack) (Zügner & Günnemann, 2019), the projected randomized block coordinate descent (PR-BCD) attack (Geisler et al., 2021), and the greedy randomized block coordinate descent (GR-BCD) attack (Geisler et al., 2021) poison the graph structure by adding new edges or deleting existing edges, resulting in changes in the properties of the underlying graph. Nodes belonging to the train set are referred to as the *train nodes*, while *test nodes* are those belonging to the test set. Our analysis shows that the PGD attack and MetaAttack introduce most edge modifications around the train nodes (Li et al., 2023b) while the local structure of the test nodes is less affected. Moreover, for homophilic graphs, adversarial edges are often introduced between nodes with dissimilar features. In contrast, for heterophilic graphs, adversarial edges are introduced between nodes with dissimilar neighborhood structures. We leverage this information to formulate a new loss function that better guides the pruning of the adversarial edges in the graph and the GNN weights. Additionally, we use self-learning to train the pruned GNNs on sparse graph structures, which improves the classification accuracy of the GLTs. To the best of our knowledge, this is the first study on the adversarial robustness of GLTs.

Our proposal is evaluated across various GNN architectures on both homophilic (Cora, citeseer, PubMed, OGBN-ArXiv, OGBN-Products) and heterophilic (Chameleon, Squirrel) graphs attacked by the PGD attack, MetaAttack, the PR-BCD attack (Geisler et al., 2021), and the GR-BCD attack for the node classification task. In case of homophilic graphs, connected nodes generally have similar features and often belong to the same class while for heterophilic graphs, linked nodes have dissimilar features and different classes. We also evaluate the proposed technique for adaptive attacks. By iteratively applying ARGS, ARGLTs can be broadly located across the 7 graph datasets with substantially reduced inference costs (up to 98% multiply-and-accumulate savings) and little to no accuracy drop. Figure 1 shows that, for node classification on Cora attacked by the PGD attack, our ARGLT achieves similar accuracy to that of the full models and graphs even with high graph and model sparsity of 48.68% and 94.53%, respectively. Compared to the GLTs identified by UGS, our ARGLTs on average achieve the same accuracy with 2.4× higher graph sparsity and 2.3× higher model sparsity.

2 Related Work

2.1 Graph Lottery Ticket Hypothesis

The lottery ticket hypothesis (LTH) (Frankle & Carbin, 2018) conjectures that there exist small sub-networks, dubbed as lottery tickets (LTs), within a dense randomly initialized network, that can be trained in isolation to achieve comparable accuracy to their dense counterparts. UGS made it possible to extend the LTH to GNNs (Chen et al., 2021), showing the existence of GLTs that can make GNN inference efficient. A GNN sub-network along with a sparse input graph is defined as a GLT if the sub-network with the original initialization trained on the sparsified graph has a matching test accuracy to the original unpruned GNN trained on the full graph. Specifically, during end-to-end training, UGS applies two differentiable binary mask tensors to the adjacency matrix and the GNN model weights, respectively. After training, the lowest-magnitude elements

are removed and the corresponding mask location is updated to 0, eliminating the low-scored edges and weights from the adjacency matrix and the GNN, respectively. The sparse GNN weight parameters are then rewound to their original initialization. To identify the GLTs, the UGS algorithm is applied in an iterative fashion until pre-defined graph and weight sparsity levels are reached. Experimental results show that UGS can significantly trim down the inference computational cost without compromising predictive accuracy. In this work, we aim to find GLTs for datasets that have been adversarially perturbed. When we apply the UGS algorithm directly to the perturbed graphs, the performance accuracy of the GLTs is substantially low compared to their clean counterparts, calling for new methods to find adversarially robust GLTs.

2.2 Adversarial Attacks on Graphs

Adversarial attacks on graphs can be classified as poisoning attacks, perturbing the graph at train time, and evasion attacks, perturbing the graph at test time. Both poisoning and evasion attacks can be targeted or global attacks (Liu et al., 2019). A targeted attack deceives the model to misclassify a specific node (Zügner et al., 2018; Bojchevski & Günnemann, 2019). A global attack degrades the overall performance of the model (Zügner & Günnemann, 2019; Wu et al., 2019). Depending on the amount of information available, the existing attacks can be categorized into white-box attacks, practical black-box attacks, and restricted black-box attacks (Zügner et al., 2018; Chang et al., 2020). An attacker can modify the node features, the discrete graph structure, or both. Different attacks show that structure perturbation is often more effective when compared to modifying the node features. Examples of global poisoning attacks include the MetaAttack (Zügner & Günnemann, 2019), PGD attack (Wu et al., 2019), PR-BCD attack (Geisler et al., 2021), and GR-BCD attack (Geisler et al., 2021). Gradient-based attacks like PGD and MetaAttack treat the adjacency matrix as a parameter tensor and modify it via scaled gradient-based perturbations that aim to maximize the loss, thus resulting in degradation of the GNN prediction accuracy. PR-BCD and GR-BCD (Geisler et al., 2021) are more scalable first-order optimization attacks that can scale up to large datasets like OGBN-ArXiv, and OGBN-Products (Hu et al., 2020) respectively. Global poisoning attacks are highly effective in reducing the classification accuracy of different GNNs and are typically more challenging to counter since they modify the graph structure before training (Zhu et al., 2021a). Therefore, we consider global graph structure poisoning attacks.

2.3 Defenses on Graphs

Several approaches have been developed to combat adversarial attacks on graphs (Tang et al., 2020; Entezari et al., 2020; Zhu et al., 2019; Jin et al., 2020b; Zhang & Zitnik, 2020; Wu et al., 2019; Deng et al., 2022; Zhou et al., 2023). Many of these techniques try to improve the classification accuracy by preprocessing the graph structure, i.e., they detect the potential adversarial edges and assign lower weights to these edges, or even remove them. Jaccard-GCN (Wu et al., 2019) removes all the edges between nodes whose features exhibit a Jaccard similarity below a certain threshold. SVD-GCN (Entezari et al., 2020) replaces the adjacency matrix with a low-rank approximation, since many real-world graphs are low-rank and attacks tend to disproportionately affect the high-frequency spectrum of the adjacency matrix. ProGNN (Jin et al., 2020b) leverages low rank, sparsity, and feature smoothness properties of graphs to clean the perturbed adjacency matrix. GARNET (Deng et al., 2022) combines spectral graph embedding with probabilistic graphical models to recover the original graph topology from the perturbed graph. GNNGuard (Zhang & Zitnik, 2020) learns weights for the edges in each message passing aggregation via cosine-similarity and penalizes the adversarial edges either by filtering them out or by assigning less weight to them. Other techniques try to improve the GNN performance by enhancing model training through data augmentation (Li et al., 2022; Feng et al., 2020), adversarial training (Wu et al., 2019), self-learning (Li et al., 2023b), robust aggregate functions (Geisler et al., 2021), or by developing novel GNN layers (Zhu et al., 2019).

Differently from the approaches above, GCN-LFR (Chang et al., 2021), a spectral-based method, leverages the fact that some low-frequency components in the graph spectrum are more robust to edge perturbations and regularizes the training process of a given GCN with robust information from an auxiliary regularization network to improve the adversarial performance of GCNs. Overall, graph preprocessing tends to remove only a small fraction of edges from the adjacency matrix. Thus, the existing defense techniques often have high latency and do not scale to large graphs. We instead aim to improve the robustness of sparse GNNs with

sparse adjacency matrices to achieve computation efficiency. As robustness generally requires more non-zero parameters, yielding parameter-efficient robust GLTs remains a challenge.

3 Methodology

Notations. Let $\mathcal{G} = \{\mathcal{V}, \mathcal{E}\}$ represent an undirected graph with $|\mathcal{V}|$ nodes and $|\mathcal{E}|$ edges. The topology of the graph can be represented with an adjacency matrix $\boldsymbol{A} \in \mathbb{R}^{|\mathcal{V}|\times|\mathcal{V}|}$, where $\boldsymbol{A}_{ij} = 1$ if there is an edge $e_{i,j} \in \mathcal{E}$ between nodes v_i and v_j while $\boldsymbol{A}_{ij} = 0$ otherwise. Each node $v_i \in \mathcal{V}$ has an attribute feature vector $\boldsymbol{x}_i \in \mathbb{R}^F$, where F is the number of node features. Let $\boldsymbol{X} \in \mathbb{R}^{|\mathcal{V}|\times F}$ and $\boldsymbol{Y} \in \mathbb{R}^{|\mathcal{V}|\times C}$ denote the feature matrix and the labels of all nodes in the graph, respectively. In this paper, we will also represent a graph as a pair $\{\boldsymbol{A}, \boldsymbol{X}\}$. In the case of message-passing GNN, the representation of a node v_i is iteratively updated by aggregating and transforming the representations of its neighbors. As an example, a two-layer(Kipf & Welling, 2016) GCN can be specified as

$$\boldsymbol{Z} = f(\{\boldsymbol{A}, \boldsymbol{X}\}, \boldsymbol{\Theta}) = \mathcal{S}(\hat{\boldsymbol{A}}\sigma(\hat{\boldsymbol{A}}\boldsymbol{X}\boldsymbol{W}_0)\boldsymbol{W}_1), \tag{1}$$

where $\boldsymbol{Z}$ is the prediction, $\boldsymbol{\Theta} = (\boldsymbol{W}_0, \boldsymbol{W}_1)$ are the weights, $\sigma(.)$ is the activation function, e.g., a rectified linear unit (ReLU), $\mathcal{S}(.)$ is the softmax function, $\hat{\boldsymbol{A}} = \tilde{\boldsymbol{D}}^{-\frac{1}{2}}(\boldsymbol{A} + \boldsymbol{I})\tilde{\boldsymbol{D}}^{-\frac{1}{2}}$ is the normalized adjacency matrix with self-loops, and $\tilde{\boldsymbol{D}}$ is the degree matrix of $\boldsymbol{A} + \boldsymbol{I}$. We consider the transductive semi-supervised node classification (SSNC) task for which the cross-entropy (CE) loss over labeled nodes is given by

$$\mathcal{L}_0(f(\{\boldsymbol{A}, \boldsymbol{X}\}, \boldsymbol{\Theta})) = -\sum_{l\in\mathcal{Y}_{TL}}\sum_{j=1}^{C}\boldsymbol{Y}_{l_j}\log(\boldsymbol{Z}_{l_j}), \tag{2}$$

where $\mathcal{Y}_{TL}$ is the set of train node indices, C is the total number of classes, and $\boldsymbol{Y}_l$ is the one-hot encoded label of node v_l.

Graph Lottery Tickets. A GLT consists of a sparsified graph, obtained by pruning some edges in $\mathcal{G}$, and a GNN sub-network, with the original initialization, that can be trained to achieve comparable performance to the original GNN trained on the full graph, where performance is measured in terms of test accuracy. Given a GNN $f(\cdot, \boldsymbol{\Theta})$ and a graph $\mathcal{G} = \{\boldsymbol{A}, \boldsymbol{X}\}$, the associated GNN sub-network and the sparsified graph can be represented as $f(\cdot, \boldsymbol{m}_\theta \odot \boldsymbol{\Theta})$ and $\mathcal{G}_s = \{\boldsymbol{m}_g \odot \boldsymbol{A}, \boldsymbol{X}\}$, respectively, where $\boldsymbol{m}_g$ and $\boldsymbol{m}_\theta$ are differentiable masks applied to the adjacency matrix $\boldsymbol{A}$ and the model weights $\boldsymbol{\Theta}$, respectively, and $\odot$ is the element-wise product. UGS (Chen et al., 2021) finds the two masks $\boldsymbol{m}_g$ and $\boldsymbol{m}_\theta$ such that the sub-network $f(\cdot, \boldsymbol{m}_\theta \odot \boldsymbol{\Theta})$ along with the sparsified graph $\mathcal{G}_s$ can be trained to a similar accuracy as $f(., \boldsymbol{\Theta})$.

Poisoning Attack on Graphs. In this work, we primarily investigate the robustness of GLTs under non-targeted poisoning attacks modifying the structure of the graph. In the case of a poisoning attack, GNNs are trained on a graph that attackers maliciously modify. The aim of the attacker is to find an optimal perturbed $\boldsymbol{A}^{'}$ that fools the GNN into making incorrect predictions. This can be formulated as a bi-level optimization problem (Zügner et al., 2018; Zügner & Günnemann, 2019):

$$\begin{aligned} &\arg\max_{\boldsymbol{A}^{'}\in\Phi(\boldsymbol{A})} \mathcal{L}_{atk}(f(\{\boldsymbol{A}^{'}, \boldsymbol{X}\}, \boldsymbol{\Theta}^*)) \\ \text{s.t.} \quad &\boldsymbol{\Theta}^* = \arg\min_{\boldsymbol{\Theta}} \mathcal{L}_0(f(\{\boldsymbol{A}^{'}, \boldsymbol{X}\}, \boldsymbol{\Theta})) \end{aligned} \tag{3}$$

where $\Phi(\boldsymbol{A})$ is the set of adjacency matrices that fit the constraint $\frac{||\boldsymbol{A}^{'} - \boldsymbol{A}||_0}{||\boldsymbol{A}||_0} \leq \Delta$, $\mathcal{L}_{atk}$ is the attack loss function, Δ is the perturbation rate, and $\boldsymbol{\Theta}^*$ is the optimal parameter for the GNN on the perturbed graph.

3.1 UGS Analysis Under Adversarial Attacks

We perform MetaAttack (Zügner & Günnemann, 2019) and the PGD attack (Wu et al., 2019) on the Cora and citeseer datasets with different perturbation rates. We use the same setup as Xu et al. (2018), Zhang & Zitnik (2020), and Mujkanovic et al. (2022) for performing the poisoning attacks on the datasets. Then, we apply UGS on these perturbed graphs to find the GLTs. As shown in Figure 2, the classification accuracy of

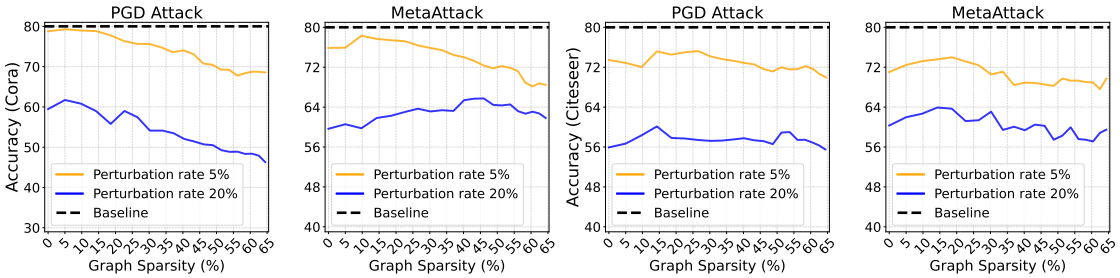

Figure 2: Classification accuracy of GLTs generated using UGS for Cora and citeseer datasets attacked by the PGD attack and MetaAttack. The baseline refers to accuracy on the clean graph.

the GLTs identified by UGS is lower than the clean graph accuracy. The difference increases substantially when the perturbation rate increases. For example, in the PGD attack, when the graph sparsity is 30%, at 5% perturbation, the accuracy drop is 6%. This drop increases to 25% when the perturbation rate is 20%. Moreover, for 20% perturbation rate, even with 0% sparsity, the accuracy of the GNN is around 20% lower than that of the clean graph accuracy. While UGS removes edges from the perturbed adjacency matrix, as shown in Figure 2, it may not effectively remove the adversarially perturbed edges. A naïve application of UGS may not be sufficient to improve the adversarial robustness of the GLTs. Consequently, there is a need for an adversarially robust UGS technique that can efficiently remove the edges affected via adversarial perturbations while pruning the adjacency matrix and the associated GNN, along with improved adversarial training, allowing the dual benefits of improved robustness and inference efficiency.

3.2 Analyzing the Impact of Adversarial Attacks on Graph Properties

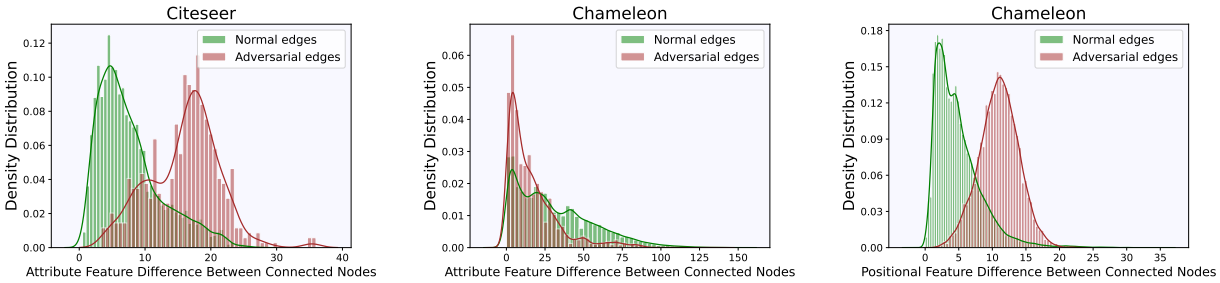

(a) (b) (c)

Figure 3: Impact of adversarial attacks on graph properties. (a), (b) Density distribution of attribute feature differences of connected nodes in perturbed homophilic (Citeseer) and heterophilic (Chameleon) graphs. (c) Density distribution of positional feature differences of connected nodes in perturbed heterophilic graphs.

Adversarial attacks like MetaAttack, PGD, PR-BCD, and GR-BCD poison the graph structure by either introducing new edges or deleting existing edges, resulting in changes in the original graph properties. We analyze the difference in the attribute features of the nodes that are connected by the clean and adversarial edges. Figure 3a and b depict the density distribution of the attribute feature difference of connected nodes in homophilic and heterophilic graph datasets attacked by the PGD attack. In homophilic graphs, the attack tends to connect nodes with large attribute feature differences. A defense technique can potentially leverage this information to differentiate between the benign and adversarial edges in the graph. However, this is not the case for heterophilic graphs. We resort, instead, to the positional features of the nodes, using positional encoding techniques like DeepWalk (Perozzi et al., 2014). Interestingly, as we observe from Figure 3c, in heterophilic graphs, attacks tend to connect nodes with large positional feature differences. ARGS uses these graph properties to iteratively prune the adversarial edges from homophilic and heterophilic graphs.

3.3 Adversarially Robust Graph Sparsification

We present ARGS, a sparsification technique that simultaneously reduces edges in $\mathcal{G}$ and GNN parameters in $\boldsymbol{\Theta}$ under adversarial attack conditions to effectively accelerate GNN inference yet maintain robust classification accuracy. ARGS reformulates the loss function to include (a) a CE loss term on the train nodes, (b) a CE loss term on a set of test nodes, and (c) a square loss term on all edges. Pruning the edges based on this combined loss function results in the removal of adversarial as well as less-important non-adversarial edges from the graph.

Removing Edges Around Train Nodes. Poisoning attacks like the MetaAttack and the PGD attack tend to modify more the local structure around the train nodes than that around the test nodes (Li et al., 2023b). Specifically, a large portion of the modifications is introduced to the edges connecting a train node to a test node or a train node to another train node. We include a CE loss term associated with the train nodes, as defined in equation 2 in our objective function to account for the edges surrounding the train nodes. These edges include both adversarial and non-adversarial edges.

Removing Adversarial Edges. In numerous application domains, including social graphs, web page graphs, and citation graphs, connected nodes in a homophilic graph exhibit similar attribute features, while they still keep similar positional features in heterophilic graphs (Li et al., 2022; McPherson et al., 2001; Kipf & Welling, 2016). On the other hand, as shown in Figure 3, adversarial attacks tend to connect nodes with distinct attribute features in homophilic graphs and distinct positional features in heterophilic graphs. Therefore, we help remove adversarial edges and encourage feature smoothness by including the following loss to our objective function for homophilic graphs:

$$\mathcal{L}_{fs}(\boldsymbol{A}^{'}, \boldsymbol{X}) = \frac{1}{2} \sum_{i,j=1} \boldsymbol{A}^{'}_{ij} (\boldsymbol{x_i} - \boldsymbol{x_j})^2, \tag{4}$$

where $\boldsymbol{A}^{'}$ is the perturbed adjacency matrix and $(\boldsymbol{x}_i - \boldsymbol{x}_j)^2$ measures the attribute feature difference. For heterophilic graphs, we introduce instead the following loss term:

$$\mathcal{L}_{fs}(\boldsymbol{A}^{'}) = \frac{1}{2} \sum_{i,j=1} \boldsymbol{A}^{'}_{ij} (\boldsymbol{y_i} - \boldsymbol{y_j})^2, \tag{5}$$

where $\boldsymbol{y}_i, \boldsymbol{y}_j \in \mathbb{R}^P$ are the positional features of nodes i, j, obtained by running the DeepWalk algorithm (Perozzi et al., 2014) on the input graph $\mathcal{G}$, P is the number of node positional features, and $(\boldsymbol{y}_i - \boldsymbol{y}_j)^2$ measures the positional feature distance.

Removing Edges Around Test Nodes. Removal of edges tends to be random in later iterations of UGS (Hui et al., 2023) since only a fraction of edges in $\mathcal{G}$ is related to the train nodes and directly impacts the corresponding CE loss. To better guide the edge removal around the test nodes, we also introduce a CE loss term for these nodes. However, the labels of the test nodes are unknown. We can then leverage the fact that structure poisoning attacks modify only the structure surrounding the train nodes, while their features and labels remain clean. Therefore, we first train a simple multi-layer perceptron (MLP) with 2 layers on the train nodes. MLPs only use the node features for training. We then use the trained MLP to predict the labels for the test nodes. We call these labels *pseudo-labels*. Finally, we use the test nodes for which the MLP has high prediction confidence for computing the test node CE loss term. Let $\mathcal{Y}_{PL}$ be the set of test nodes for which the MLP prediction confidence is high and $\boldsymbol{Y}_{mlp}$ be the prediction by the MLP. The CE loss

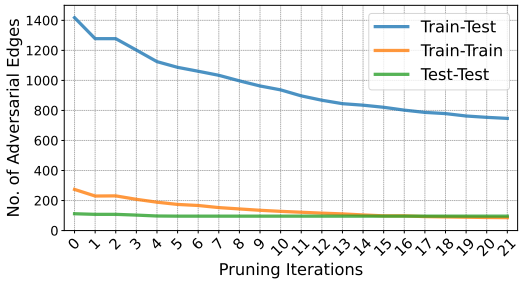

Figure 4: Evolution of adversarial edges in Cora dataset (attacked by PGD, 20% perturbation) as we apply ARGS to prune the graph. Train-Train edges connect two nodes from the train set. Train-Test edges connect a node from train set with one from test set. Test-Test edges connect two nodes from the test set.

Algorithm 1 Adversarially Robust Graph Sparsification

Input: Graph $\mathcal{G} = \{\boldsymbol{A}, \boldsymbol{X}\}$, GNN $f(\mathcal{G}, \boldsymbol{\Theta}_0)$ with initialization $\boldsymbol{\Theta}^0$, Sparsity levels s_g for graph and s_θ for GNN, Initial masks $\boldsymbol{m}_g = \boldsymbol{A}$, $\boldsymbol{m}_\theta = 1 \in \mathbb{R}^{||\boldsymbol{\Theta}_0||_0}$

Output: Final masks $\boldsymbol{m}_g$, $\boldsymbol{m}_\theta$

while $\left(1 - \frac{||\boldsymbol{m}_g||_0}{||\boldsymbol{A}||_0} < s_g\right)$ and $\left(1 - \frac{||\boldsymbol{m}_\theta||_0}{||\boldsymbol{\Theta}||_0} < s_\theta\right)$ **do**
  $\boldsymbol{m}_g^{(0)} = \boldsymbol{m}_g$, $\boldsymbol{m}_\theta^{(0)} = \boldsymbol{m}_\theta$, $\boldsymbol{\Theta}^{(0)} = \{\boldsymbol{W}_0^{(0)}, \boldsymbol{W}_1^{(0)}\}$
  for $t = 0, 1, 2, \ldots, T-1$ **do**
    Input $\mathcal{G} = \{\boldsymbol{m}_g^t \odot \boldsymbol{A}, \boldsymbol{X}\}$ to $f(\cdot, \boldsymbol{m}_\theta^t \odot \boldsymbol{\Theta}^t)$ to compute the loss $\mathcal{L}_{ARGS}$ in equation equation 7
    $\boldsymbol{\Theta}^{t+1} \leftarrow \boldsymbol{\Theta}^t - \mu \nabla_{\boldsymbol{\Theta}^t} \mathcal{L}_{ARGS}$
    $\boldsymbol{m}_g^{t+1} \leftarrow \boldsymbol{m}_g^t - \omega_g \nabla_{\boldsymbol{m}_g^t} \mathcal{L}_{ARGS}$
    $\boldsymbol{m}_\theta^{t+1} \leftarrow \boldsymbol{m}_\theta^t - \omega_\theta \nabla_{\boldsymbol{m}_\theta^t} \mathcal{L}_{ARGS}$
  $\boldsymbol{m}_g = \boldsymbol{m}_g^{T-1}$, $\boldsymbol{m}_\theta = \boldsymbol{m}_\theta^{T-1}$
  Set percentage p_g of the lowest-scored values in $\boldsymbol{m}_g$ to 0 and set others to 1
  Set percentage p_θ of the lowest-scored values in $\boldsymbol{m}_\theta$ to 0 and set others to 1

is given by

$$\mathcal{L}_1(f(\{\boldsymbol{A}^{'}, \boldsymbol{X}\}, \boldsymbol{\Theta})) = -\sum_{l \in \mathcal{Y}_{TL}} \sum_{j=1}^{C} \boldsymbol{Y}_{mlp_{l_j}} \log(\boldsymbol{Z}_{l_j}). \tag{6}$$

In summary, the complete loss function that ARGS optimizes is

$$\begin{aligned} \mathcal{L}_{ARGS} = \alpha \mathcal{L}_0(f(\{\boldsymbol{m}_g \odot \boldsymbol{A}^{'}, \boldsymbol{X}\}, \boldsymbol{m}_\theta \odot \boldsymbol{\Theta})) + \beta \mathcal{L}_{fs}(\boldsymbol{m}_g \odot \boldsymbol{A}^{'}, \boldsymbol{X}) \\ + \gamma \mathcal{L}_1(f(\{\boldsymbol{m}_g \odot \boldsymbol{A}^{'}, \boldsymbol{X}\}, \boldsymbol{m}_\theta \odot \boldsymbol{\Theta})) + \lambda_1 ||\boldsymbol{m}_g||_1 + \lambda_2 ||\boldsymbol{m}_\theta||_1, \end{aligned} \tag{7}$$

where β, λ_1, and λ_2 are the hyperparameters and the value of α and γ is set to 1. λ_1 and λ_2 are the l_1 regularizers of $\boldsymbol{m}_g$ and $\boldsymbol{m}_\theta$, respectively. After the training is complete, the lowest percentages p_g of elements of $\boldsymbol{m}_g$ and p_θ of elements of $\boldsymbol{m}_\theta$ are set to 0. Then, the updated masks are applied to prune $\boldsymbol{A}$ and $\boldsymbol{\Theta}$, and the weights of the GNN are rewound to their original initialization value to generate the ARGLT. We apply these steps iteratively until we reach the desired sparsity s_g and s_θ. Algorithm 1 illustrates our iterative pruning process, where $|| \cdot ||_0$ is the L_0 norm, counting the number of non-zero elements. As shown in Figure 4 for the Cora dataset attacked by the PGD attack with 20% perturbation, most of the adversarial perturbation edges are between train and test nodes (Li et al., 2023b). Moreover, our proposed sparsification technique successfully removes many of the adversarial edges. In particular, after applying our technique for 20 iterations, where each iteration removes 5% of the graph edges, the number of train-train, train-test, and test-test adversarial edges reduces by 68.13%, 47.3%, and 14.3%, respectively.

Training Sparse ARGLTs. Structure poisoning attacks do not modify the labels of the nodes. In the case of attacks like PGD and MetaAttack, the locality structure of the test nodes is less contaminated (Li et al., 2023b), implying that the train node labels and the local structure of the test nodes contain relatively "clean" information. We leverage this insight and train the GNN sub-network using both train nodes and test nodes. We use a CE loss term for both the train ($\mathcal{L}_0$) and test ($\mathcal{L}_1$) nodes. Since the true labels of the test nodes are not available, we train an MLP on the train nodes and then use it to predict the labels for the test nodes (Li et al., 2018; 2023b). To compute the CE loss, we use only those test nodes for which the MLP has high prediction confidence. The loss function used for training the sparse GNN on the sparse adjacency matrix generated by ARGS is

$$\min_{\boldsymbol{\Theta}} \quad \eta \mathcal{L}_0(f(\{\boldsymbol{m}_g \odot \boldsymbol{A}^{'}, \boldsymbol{X}\}, \boldsymbol{m}_\theta \odot \boldsymbol{\Theta})) + \zeta \mathcal{L}_1(f(\{\boldsymbol{m}_g \odot \boldsymbol{A}^{'}, \boldsymbol{X}\}, \boldsymbol{m}_\theta \odot \boldsymbol{\Theta})) \tag{8}$$

where $\boldsymbol{m}_\theta$ and $\boldsymbol{m}_g$ are the masks evaluated by ARGS that are kept fixed throughout training, and η is set to 1. In the early pruning iterations, when graph sparsity is low, the test nodes are more useful in improving the model adversarial performance because the train nodes' localities are adversarially perturbed and there exist distribution shifts between the train and test nodes. However, as the graph sparsity increases, adversarial edges associated with the train nodes are gradually removed by ARGS, thus reducing the distribution shift and making the contribution of the train nodes more important in the adversarial training.

4 Evaluation

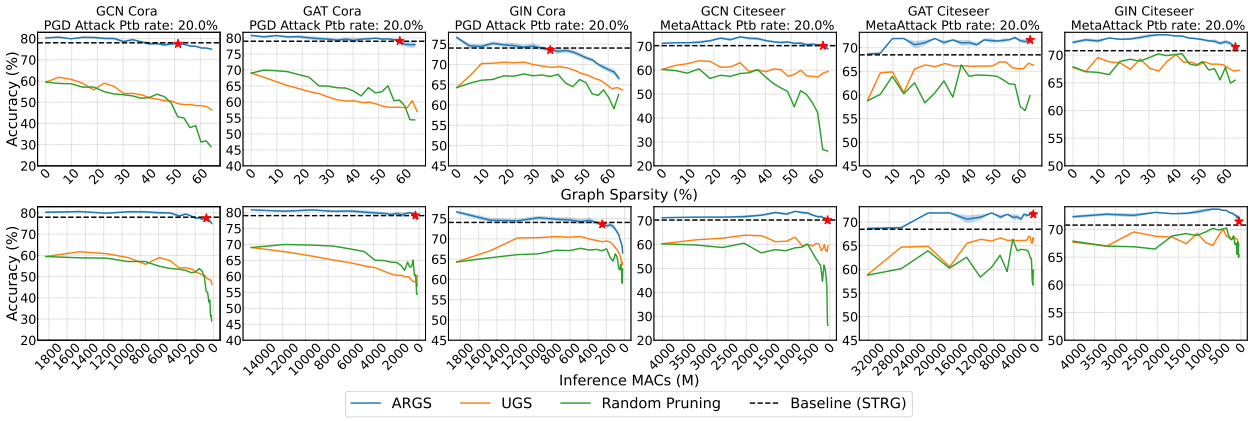

Figure 5: Node classification performance versus graph sparsity levels and inference MACs for the GCN, GIN, and GAT architectures on Cora and Citeseer datasets attacked by PGD and MetaAttack, respectively. Red stars ⋆ indicate the ARGLTs. Dash black lines represent the performance of STRG, an adversarial defense technique.

4.1 Evaluation Setup

We evaluate the effectiveness of ARGS and the existence of ARGLTs across diverse datasets and GNN models under different adversarial attacks and perturbation rates. In particular, we evaluate our sparsification method on both homophilic and heterophilic graph datasets which are attacked by two structure poisoning attacks, namely, PGD (Wu et al., 2019) and MetaAttack (Zügner & Günnemann, 2019). We also evaluate ARGS on a large dataset, namely, OGBN-ArXiv and OGBN-Products (Hu et al., 2020) attacked by the PR-BCD and GR-BCD attacks, respectively. Finally, we evaluate the robustness of ARGS against adaptive attacks (Mujkanovic et al., 2022). We compare our method with UGS (Chen et al., 2021), random pruning, and other state-of-the-art adversarial defense methods, namely, STRG (Li et al., 2023b), GARNET (Deng et al., 2022), GNNGuard (Zhang & Zitnik, 2020), ProGNN (Jin et al., 2020a), and Soft Median (Geisler et al., 2021). Only UGS and random pruning techniques prune both the graph adjacency matrix and the GNN model parameters – no other existing defense techniques prune the GNN model parameters. For a fair comparison, we set $p_g = 5\%, p_\theta = 20\%$, similarly to the parameters used by UGS. More details on the dataset statistics, model configurations, and hyperparameters in ARGS can be found in Appendix A.1.

4.2 Defense on Homophilic Graphs

We first evaluate the performance of ARGS on homophilic graphs against PGD and MetaAttack. Due to space limitations, we show the results for a 20% perturbation rate for the Cora and Citeseer datasets. Results for PubMed and other perturbation rates are shown in Appendix A.3. We consider 3 different backbones, namely, graph convolution networks (GCNs) (Kipf & Welling, 2016), graph isomorphism networks (GINs) (Xu et al., 2018), and graph attention networks (Veličković et al., 2017). Figure 5 shows the results for the GCN, GIN, and GAT architectures on the Cora and Citeseer datasets attacked by PGD and MetaAttack, respectively, where the average accuracy of ARGLT is reported across 5 runs. ARGLTs at a range of graph sparsity from 30% to 60% with similar performance as the STRG baseline can be identified across the different GNN backbones. The ARGLTs significantly reduce the inference MACs for GCN, GIN, and GAT by $\sim 95\%, \sim 97\%$, and $\sim 83\%$, respectively, for the Cora dataset. For the Citeseer dataset, the inference MACs reduce by $\sim 98\%$ for all the backbone GNNs.

Comparison with Other Defense Techniques. We compare the performance of ARGS with GNNGuard, GARNET, and ProGNN, which are all defense methods. Differently from ARGS, none of these methods prunes the weights of the GNN model. We compare these methods in terms of accuracy and inference MAC and we consider GCN as the backbone. For the different baselines, the GLT which has similar accuracy as

Table 1: Performance comparison between ARGS and other defense techniques in terms of accuracy and inference MAC count

	Cora (PGD attack) Perturbation Rate 20%		Citeseer (MetaAttack) Perturbation Rate 20%	
Model	Accuracy (%)	Inference MACs (M)	Accuracy (%)	Inference MACs (M)
GCN-ProGNN	63.43±0.89	1832.14	61.02 ±0.11	4006.91
GCN-ARGS	**77.53±1.15**	**78.78**	**68.97 ±0.89**	**43.78**
GCN-GNNGuard	73.19±0.72	1948.32	71.62±1.01	4188.33
GCN-ARGS	**77.53±1.15**	**78.78**	**71.78±0.58**	**211.77**
GCN-GARNET	66.66±1.10	1684.9	72.97±1.20	3898.21
GCN-ARGS	**77.53±1.15**	**78.78**	**73.19±0.78**	**425.81**

the baseline with maximum graph and model sparsity is identified as the ARGLT by ARGS and reported in Table 1. For the Cora dataset, the ARGLT identified by ARGS for PGD attack (20% perturbation rate) with maximum sparsity levels (model sparsity: 98.9%, graph sparsity: 64.1%) has a classification accuracy of 77.53%. The three different defense techniques, namely, ProGNN, GNNGuard, and GARNET have a classification accuracy of 63.43%, 73.19%, and 66.66%, respectively, which are all less than the classification accuracy of the most sparse ARGLT identified by ARGS. Therefore, when comparing these different defense techniques, we report the performance of the ARGLT with maximum sparsity level in Table equation 1. For the Citeseer dataset attacked by MetaAttack with a 20% perturbation rate, the most sparse ARGLT has a classification accuracy of 70.2%. The defense technique ProGNN has a classification accuracy of 61.02%, which is less than the classification accuracy of the most sparse ARGLT. Hence, we compare it with the most sparse ARGLT. The defense techniques GNNGuard and GARNET have a classification accuracy of 71.62% and 72.97%, respectively. In these cases, the GLT with the same classification accuracy as the defense technique is reported in Table equation 1.

4.3 Defense on Large Graphs

We evaluate the robustness of ARGS on the large-scale datasets OGBN-ArXiv and OGBN-Products. OGBN-ArXiv has 170,000 nodes and 1.16 million edges while OGBN-Products has 2.5 million nodes and 61 million edges. We use the PR-BCD attack for perturbing the OGBN-ArXiv dataset. Attempting the PR-BCD attack on the OGBN-Products dataset resulted in out-of-memory errors. We then conducted a more scalable GR-BCD attack (Geisler et al., 2021) on the OGBN-Products dataset, employing a perturbation rate of 50%. The reference GNN model is Deeper-GCN (Li et al., 2023a). For both the PR-BCD and GR-BCD attacks, the adversarial edges are uniformly distributed among the train and test nodes. Hence, we set the value of ζ to be 0. The PGD attack or MetaAttack faces timeout due to memory for these large graphs. Figure 6 shows that ARGS can identify ARGLTs that have high model and graph sparsity compared to UGS. Here we take GARNET as the baseline. In particular, the model sparsity and graph sparsity are 96.48% and 53.68% for the 10% perturbed dataset, and 97.19% and 55.99%, respectively, for the 15% perturbed dataset. Results on the OGBN-Products dataset are reported in Table 2. Our baselines include GCN, GARNET, GNNGuard, and Soft Median GDC. For the different baselines, the GLT which has similar accuracy as the baseline with maximum graph and model sparsity is identified as the ARGLT by ARGS and reported in Table 2. Here we compare

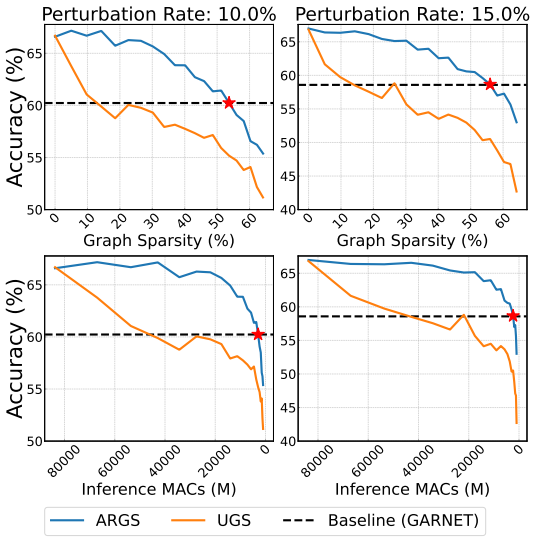

Figure 6: Node classification performance versus graph sparsity levels and inference MACs for Deeper-GCN on OGBN-ArXiv dataset attacked by PR-BCD.

Table 2: Comparison between ARGLTs identified by ARGS and GLTs identified by UGS in terms of Graph sparsity, Model sparsity, and Inference MACs across different baselines for the OGBN-Products dataset

Baseline	**Accuracy (%)**	**Graph Sparsity(%)**		**Model Sparsity(%)**		**Inference MACs(M)**	
		UGS	ARGS	UGS	ARGS	UGS	ARGS
Soft Median GDC	59.23	87.84	87.84	87.89	87.89	75721.5	75727.8
GCN	62.71	83.32	**87.84**	83.36	**87.89**	104076.4	**75727.8**
GNNGuard	63.22	83.32	**87.84**	83.36	**87.89**	104076.4	**75727.8**
GARNET	74.97	19.00	**40.95**	19.01	**40.98**	506511.0	**369089.2**

Table 3: ARGS and UGS performance comparison for the PGD attack and an adaptive attack for the Cora dataset. GCN is used as the GNN model.

			Classification Accuracy at Perturbation Rate 5%		Classification Accuracy at Perturbation Rate 10%	
Dataset	Technique	Attack	Graph Sparsity 22.64% Model Sparsity 67.60%	Graph Sparsity 43.16% Model Sparsity 91.70%	Graph Sparsity 22.64% Model Sparsity 67.60%	Graph Sparsity 43.16% Model Sparsity 91.70%
Cora	UGS	PGD Attack	75.95±0.19	72.11±0.40	69.48±0.28	66.18±0.13
		Adaptive Attack	74.13±0.20	70.98±0.33	68.02±0.45	64.79±0.34
Cora	ARGS	PGD Attack	**82.04±1.09**	**80.68±0.85**	**82.8±0.77**	**80.18±1.13**
		Adaptive Attack	**80.33±1.35**	**78.77±1.86**	**79.68±1.35**	**77.16±0.98**
Citeseer	UGS	PGD Attack	74.63±0.30	72.29±0.36	70.70±0.26	69.34±0.49
		Adaptive Attack	69.8±0.31	66.97±0.25	65.48±0.31	63.98±0.18
Citeseer	ARGS	PGD Attack	**75.32±0.88**	**74.17±0.56**	**74.7±0.98**	**73.53±.1.05**
		Adaptive Attack	**74.11±1.76**	**73.16±0.87**	**72.93±1.87**	**71.89±1.01**

the performance between UGS and ARGS and as evident from Table 2, ARGS can identify lottery tickets with higher graph and model sparsity than UGS.

4.4 Defense Against Adaptive Attacks.

Recently, adaptive attacks (Mujkanovic et al., 2022) have been developed, which are targeted to specific defense techniques, to evaluate their robustness. Because all the components in the loss function of ARGS are differentiable, ARGS can also be directly attacked by an adaptive attack. Specifically, we evaluate ARGS on a gradient-based adaptive attack, called Meta-PGD (Mujkanovic et al., 2022), where ARGS is attacked by unrolling its training procedure. Table 3 compares the performance of ARGS against the PGD attack and the adaptive attack, with GCN as the GNN backbone for Cora and CiteSeer. For a 5% perturbation rate, the accuracy of the ARGLT identified by ARGS reduces by only ∼1.7% for Cora while for CiteSeer it reduces by only ∼1.5%. For a 10% perturbation rate, the reduction in classification accuracy is ∼2.9% for the Cora dataset and ∼2.5% for the Cora dataset, showing that ARGS is also robust to adaptive attacks. Table 3 shows that the classification accuracy of the ARGLTs is on average 9% more than the GLTs identified by UGS for Cora and 6% for CiteSeer, respectively.

4.5 Defense on Heterophilic Graphs.

We report the classification accuracy of ARGS on heterophilic graphs in Figure 7. We use GPRGNN (Chien et al., 2020) as the GNN model for the heterophilic graph datasets Chameleon and Squirrel (McCallum et al., 2000). GPRGNN performs better than GCN, GIN, and GAT for heterophilic graphs (Deng et al., 2022). We use GARNET as the baseline since it achieves state-of-the-art adversarial classification accuracy compared to other defense techniques for heterophilic graphs. As shown in Figure 7, ARGS is able to identify GLTs that achieve similar classification accuracy as GARNET for the Chameleon and Squirrel datasets attacked by PGD and MetaAttack with 85% to 97% weight sparsity, resulting in a substantial reduction in inference MACs.

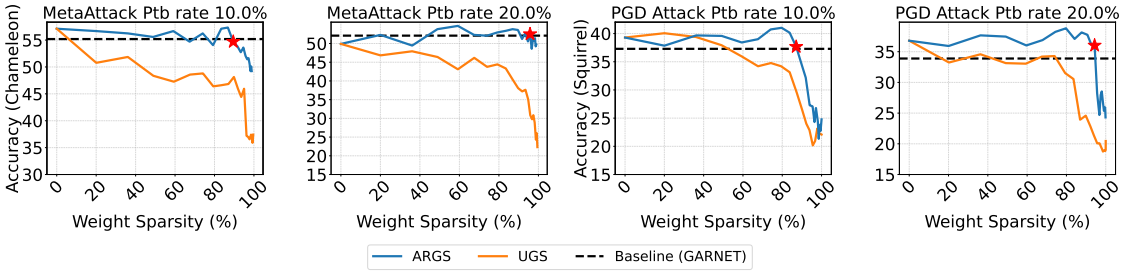

Figure 7: Node classification performance versus weight sparsity levels for GPRGNN on Chameleon and Squirrel dataset attacked by the PGD Attack and MetaAttack.

4.6 Analysis Under Structure and Node Feature Attacks.

In addition to structural attacks, we also evaluate the performance of ARGS against an attack that modifies both the graph structure and the node features simultaneously. Mettack (Zügner & Günnemann, 2019) can be modified for this purpose. For a given perturbation budget, this attack performs a structure perturbation and a feature perturbation at each iteration, and between the two perturbations, it chooses the one that results in a higher attack loss. This iterative process is repeated until the perturbation budget is exhausted. We attack the Cora and Citeseer datasets with 5%, 10%, and 15% perturbation rates, and use the STRG defense technique as the baseline. ARGS can find highly sparse GLTs that achieve similar classification accuracy as the baseline for different graph datasets perturbed with different perturbation rates using this attack. For example, for a 5% perturbation rate, ARGS finds GLTs that have 53.75% graph sparsity and 96.55% model sparsity for the Cora dataset and 58.31% graph sparsity and 97.92% model sparsity for the Citeseer dataset. We also include the performance of UGS for comparison. Figure 8 shows that, for the same sparsity levels, GLTs identified by ARGS achieve much higher classification accuracy when compared to GLTs identified by UGS. We observe that the attacked graph contains more edge perturbations than feature perturbations since modifying the graph structure results in higher attack loss than modifying the node features. This result shows that ARGS can find highly sparse GLTs for graphs attacked by both structure and node feature perturbations.

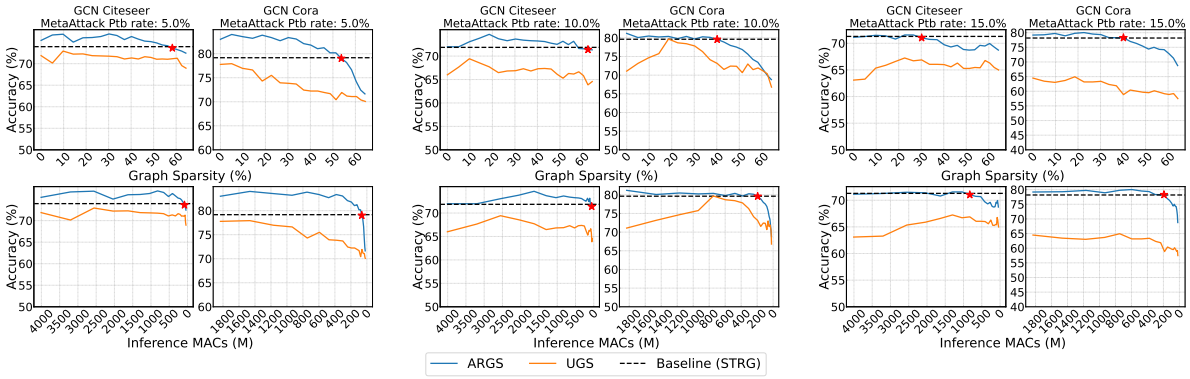

Figure 8: Node classification performance over achieved graph sparsity levels for a GCN model on Cora and Citeseer datasets attacked by a version of the MetaAttack that modifies both graph structure and node features. The perturbation rates are 5%, 10%, and 15%. Red stars ⋆ indicate the ARGLTs. STRG is used as the baseline.

4.7 Ablation Study

We evaluate the effectiveness of each component of the proposed loss function for the sparsification algorithm by performing an ablation study, as shown in Table 4. We consider the Cora dataset under PGD attack with 10% and 20% perturbation rates. Configuration 1 corresponds to ARGS with all the loss components (equation 7). Configuration 2 does not use the feature smoothness component (equation 4) while configuration

3 skips the CE loss associated with the predicted test nodes (equation 6). Configuration 4 skips both the smoothness and CE loss on predicted test nodes. Table 4 shows that both configurations 2 and 3 improve the final performance when compared to that of configuration 4, highlighting the importance of the losses introduced in equation 4 and equation 6. More importantly, at both high and low target sparsity, we yield the best classification performance with configuration 1, showcasing the importance of the unified loss function (equation 7). Further ablation studies are provided in the appendix.

Table 4: Ablation study.

GCN, Cora, PGD Attack						Classification Accuracy at Perturbation Rate 10%		Classification Accuracy at Perturbation Rate 20%	
Configuration	α	β	γ	η	ζ	Graph Sparsity 9.8% Model Sparsity 36.1%	Graph Sparsity 64.4% Model Sparsity 98.9%	Graph Sparsity 9.8% Model Sparsity 36.1%	Graph Sparsity 64.5% Model Sparsity 98.9%
1	✓	✓	✓	✓	✓	**83.25**	**75.10**	**80.63**	**75.60**
2	✓	✗	✓	✓	✓	82.04	70.57	78.92	64.84
3	✓	✓	✗	✓	✓	82.44	72.84	78.97	52.92
4	✓	✗	✗	✓	✓	80.58	62.42	75.7	54.18

5 Conclusion

In this paper, we first empirically observed that the performance of GLTs collapses against structure perturbation poisoning attacks. To address this issue, we presented a new adversarially robust graph sparsification technique, ARGS, that prunes the perturbed adjacency matrix and the GNN weights by optimizing a novel loss function. By iteratively applying ARGS, we found ARGLTs that are highly sparse yet achieve competitive performance under different structure poisoning attacks. Our evaluation showed the superiority of our method over UGS at both high and low sparsity regimes.

References

Aleksandar Bojchevski and Stephan Günnemann. Adversarial attacks on node embeddings via graph poisoning. In *International Conference on Machine Learning*, pp. 695–704. PMLR, 2019.

Heng Chang, Yu Rong, Tingyang Xu, Wenbing Huang, Honglei Zhang, Peng Cui, Wenwu Zhu, and Junzhou Huang. A restricted black-box adversarial framework towards attacking graph embedding models. In *Proceedings of the AAAI Conference on Artificial Intelligence*, volume 34, pp. 3389–3396, 2020.

Heng Chang, Yu Rong, Tingyang Xu, Yatao Bian, Shiji Zhou, Xin Wang, Junzhou Huang, and Wenwu Zhu. Not all low-pass filters are robust in graph convolutional networks. *Advances in Neural Information Processing Systems*, 34:25058–25071, 2021.

Tianlong Chen, Yongduo Sui, Xuxi Chen, Aston Zhang, and Zhangyang Wang. A unified lottery ticket hypothesis for graph neural networks. In *International Conference on Machine Learning*, pp. 1695–1706. PMLR, 2021.

Eli Chien, Jianhao Peng, Pan Li, and Olgica Milenkovic. Adaptive universal generalized pagerank graph neural network. *arXiv preprint arXiv:2006.07988*, 2020.

Hanjun Dai, Hui Li, Tian Tian, Xin Huang, Lin Wang, Jun Zhu, and Le Song. Adversarial attack on graph structured data. In *International conference on machine learning*, pp. 1115–1124. PMLR, 2018.

Chenhui Deng, Xiuyu Li, Zhuo Feng, and Zhiru Zhang. GARNET: Reduced-rank topology learning for robust and scalable graph neural networks. In *Learning on Graphs Conference*, pp. 3–1. PMLR, 2022.

Negin Entezari, Saba A Al-Sayouri, Amirali Darvishzadeh, and Evangelos E Papalexakis. All you need is low (rank) defending against adversarial attacks on graphs. In *Proceedings of the 13th International Conference on Web Search and Data Mining*, pp. 169–177, 2020.

Wenzheng Feng, Jie Zhang, Yuxiao Dong, Yu Han, Huanbo Luan, Qian Xu, Qiang Yang, Evgeny Kharlamov, and Jie Tang. Graph random neural networks for semi-supervised learning on graphs. *Advances in neural information processing systems*, 33:22092–22103, 2020.

Matthias Fey and Jan E. Lenssen. Fast graph representation learning with PyTorch Geometric. In *ICLR Workshop on Representation Learning on Graphs and Manifolds*, 2019.

Jonathan Frankle and Michael Carbin. The lottery ticket hypothesis: Finding sparse, trainable neural networks. *arXiv preprint arXiv:1803.03635*, 2018.

Simon Geisler, Tobias Schmidt, Hakan Şirin, Daniel Zügner, Aleksandar Bojchevski, and Stephan Günnemann. Robustness of graph neural networks at scale. *Advances in Neural Information Processing Systems*, 34: 7637–7649, 2021.

Will Hamilton, Zhitao Ying, and Jure Leskovec. Inductive representation learning on large graphs. *Advances in neural information processing systems*, 30, 2017.

Weihua Hu, Matthias Fey, Marinka Zitnik, Yuxiao Dong, Hongyu Ren, Bowen Liu, Michele Catasta, and Jure Leskovec. Open graph benchmark: Datasets for machine learning on graphs. *Advances in neural information processing systems*, 33:22118–22133, 2020.

Bo Hui, Da Yan, Xiaolong Ma, and Wei-Shinn Ku. Rethinking graph lottery tickets: Graph sparsity matters. *arXiv preprint arXiv:2305.02190*, 2023.

Wei Jin, Yaxin Li, Han Xu, Yiqi Wang, and Jiliang Tang. Adversarial attacks and defenses on graphs: A review and empirical study. *arXiv preprint arXiv:2003.00653*, 10(3447556.3447566), 2020a.

Wei Jin, Yao Ma, Xiaorui Liu, Xianfeng Tang, Suhang Wang, and Jiliang Tang. Graph structure learning for robust graph neural networks. In *Proceedings of the 26th ACM SIGKDD international conference on knowledge discovery & data mining*, pp. 66–74, 2020b.

Thomas N Kipf and Max Welling. Semi-supervised classification with graph convolutional networks. *arXiv preprint arXiv:1609.02907*, 2016.

Guohao Li, Chenxin Xiong, Guocheng Qian, Ali Thabet, and Bernard Ghanem. DeeperGCN: Training deeper GCNs with generalized aggregation functions. *IEEE Transactions on Pattern Analysis and Machine Intelligence*, 45(11):13024–13034, 2023a. doi: 10.1109/TPAMI.2023.3306930.

Kuan Li, Yang Liu, Xiang Ao, Jianfeng Chi, Jinghua Feng, Hao Yang, and Qing He. Reliable representations make a stronger defender: Unsupervised structure refinement for robust gnn. In *Proceedings of the 28th ACM SIGKDD Conference on Knowledge Discovery and Data Mining*, pp. 925–935, 2022.

Kuan Li, Yang Liu, Xiang Ao, and Qing He. Revisiting graph adversarial attack and defense from a data distribution perspective. In *The Eleventh International Conference on Learning Representations*, 2023b.

Qimai Li, Zhichao Han, and Xiao-Ming Wu. Deeper insights into graph convolutional networks for semi-supervised learning. In *Proceedings of the AAAI conference on artificial intelligence*, volume 32, 2018.

Yaxin Li, Wei Jin, Han Xu, and Jiliang Tang. DeepRobust: A pytorch library for adversarial attacks and defenses. *arXiv preprint arXiv:2005.06149*, 2020.

Xuanqing Liu, Si Si, Xiaojin Zhu, Yang Li, and Cho-Jui Hsieh. A unified framework for data poisoning attack to graph-based semi-supervised learning. *arXiv preprint arXiv:1910.14147*, 2019.

Andrew Kachites McCallum, Kamal Nigam, Jason Rennie, and Kristie Seymore. Automating the construction of internet portals with machine learning. *Information Retrieval*, 3:127–163, 2000.

Miller McPherson, Lynn Smith-Lovin, and James M Cook. Birds of a feather: Homophily in social networks. *Annual review of sociology*, 27(1):415–444, 2001.

Felix Mujkanovic, Simon Geisler, Stephan Günnemann, and Aleksandar Bojchevski. Are defenses for graph neural networks robust? *Advances in Neural Information Processing Systems 35 (NeurIPS 2022)*, 2022.

Bryan Perozzi, Rami Al-Rfou, and Steven Skiena. DeepWalk: Online learning of social representations. In *Proceedings of the 20th ACM SIGKDD international conference on Knowledge discovery and data mining*, pp. 701–710, 2014.

Xianfeng Tang, Yandong Li, Yiwei Sun, Huaxiu Yao, Prasenjit Mitra, and Suhang Wang. Transferring robustness for graph neural network against poisoning attacks. In *Proceedings of the 13th international conference on web search and data mining*, pp. 600–608, 2020.

Petar Veličković, Guillem Cucurull, Arantxa Casanova, Adriana Romero, Pietro Lio, and Yoshua Bengio. Graph attention networks. *arXiv preprint arXiv:1710.10903*, 2017.

Huijun Wu, Chen Wang, Yuriy Tyshetskiy, Andrew Docherty, Kai Lu, and Liming Zhu. Adversarial examples on graph data: Deep insights into attack and defense. *arXiv preprint arXiv:1903.01610*, 2019.

Keyulu Xu, Weihua Hu, Jure Leskovec, and Stefanie Jegelka. How powerful are graph neural networks? *arXiv preprint arXiv:1810.00826*, 2018.

Zhitao Ying, Jiaxuan You, Christopher Morris, Xiang Ren, Will Hamilton, and Jure Leskovec. Hierarchical graph representation learning with differentiable pooling. *Advances in neural information processing systems*, 31, 2018.

Muhan Zhang and Yixin Chen. Link prediction based on graph neural networks. *Advances in neural information processing systems*, 31, 2018.

Xiang Zhang and Marinka Zitnik. GNNGuard: Defending graph neural networks against adversarial attacks. *Advances in neural information processing systems*, 33:9263–9275, 2020.

Ziwei Zhang, Peng Cui, and Wenwu Zhu. Deep learning on graphs: A survey. *IEEE Transactions on Knowledge and Data Engineering*, 34(1):249–270, 2020.

Bingxin Zhou, Yuanhong Jiang, Yuguang Wang, Jingwei Liang, Junbin Gao, Shirui Pan, and Xiaoqun Zhang. Robust graph representation learning for local corruption recovery. In *Proceedings of the ACM Web Conference 2023*, pp. 438–448, 2023.

Jie Zhou, Ganqu Cui, Shengding Hu, Zhengyan Zhang, Cheng Yang, Zhiyuan Liu, Lifeng Wang, Changcheng Li, and Maosong Sun. Graph neural networks: A review of methods and applications. *AI open*, 1:57–81, 2020.

Dingyuan Zhu, Ziwei Zhang, Peng Cui, and Wenwu Zhu. Robust graph convolutional networks against adversarial attacks. In *Proceedings of the 25th ACM SIGKDD international conference on knowledge discovery & data mining*, pp. 1399–1407, 2019.

Jiong Zhu, Junchen Jin, Michael T Schaub, and Danai Koutra. Improving robustness of graph neural networks with heterophily-inspired designs. *arXiv preprint arXiv:2106.07767*, 3, 2021a.

Yanqiao Zhu, Weizhi Xu, Jinghao Zhang, Qiang Liu, Shu Wu, and Liang Wang. Deep graph structure learning for robust representations: A survey. *arXiv preprint arXiv:2103.03036*, 14, 2021b.

Daniel Zügner and Stephan Günnemann. Adversarial attacks on graph neural networks via meta learning. *The seventh International Conference on Learning Representations*, 2019.

Daniel Zügner, Amir Akbarnejad, and Stephan Günnemann. Adversarial attacks on neural networks for graph data. In *Proceedings of the 24th ACM SIGKDD international conference on knowledge discovery & data mining*, pp. 2847–2856, 2018.

A Appendix

A.1 Dataset Details

We use seven different benchmark datasets, namely, Cora, Citeseer, PubMed, OGBN-arXiv, OGBN-Produts, Chameleon, and Squirrel, to evaluate the efficacy of ARGS in finding ARGLTs. Details about the benchmark datasets are summarized in Table 5. In the case of Cora, Citeseer, and PubMed, 10% data constitute the train set, 10% data constitute the validation set while the test set is 80%. For Chameleon and Squirrel [39], we keep the same data split setting as Chien et al. (2020). For OGBN-ArXiv, and OGBN-Products we follow the data split setting of Open Graph Benchmark (OGB) (Hu et al., 2020).

A.2 Implementation Details

For fair comparison, we follow the setup used by UGS as our default setting (Chen et al., 2021). For Cora, Citeseer, and PubMed we conduct all our experiments on two-layer GCN, GIN, and GAT networks with 512 hidden units. The graph sparsity p_g and model sparsity p_θ are 5% and 20% unless otherwise stated. The value of β is chosen from $\{0.01, 0.1, 1, 10\}$ while the value of α, γ, η, and ζ is 1 by default. We use the Adam optimizer for training the GNNs. In each pruning round, the number of epochs to update the masks is by default 200, using early stopping. The 2-layer MLP used for predicting the pseudo-labels of the test nodes has by default hidden dimension of 1024 unless otherwise mentioned. We use DeepRobust, an adversarial attack library (Li et al., 2020), to implement the PGD attack and MetaAttack on the different datasets. We use Pytorch-Geometric (Fey & Lenssen, 2019) to perform the PR-BCD and GR-BCD attacks on the OGBN-ArXiv and OGBN-Products datasets, respectively. All the experiments are conducted on an NVIDIA Tesla A100 (80GB GPU).

For GCN, the values of λ_1 and λ_2 are 10^{-2} and 10^{-2} for Cora and Citeseer, while for PubMed they are 10^{-6} and 10^{-3}, respectively. The value of the learning rate is 8×10^{-3} and that of the weight decay is 8×10^{-5} for the Cora dataset. For Citeseer and PubMed, the learning rate is 10^{-2} and the weight decay is 5×10^{-4}. For the different datasets, we use a dropout of 0.5.

In the case of GIN, for the Cora dataset, the learning rate is 8×10^{-3}, the weight decay is 8×10^{-5}, λ_1 is 10^{-3}, and λ_2 is 10^{-3}. For Citeseer, the learning rate is 10^{-2}, the weight decay is 5×10^{-4}, λ_1 is 10^{-5}, and λ_2 is 10^{-5}. For GAT, in the case of the Cora dataset, the learning rate is 8×10^{-3}, the weight decay is 8×10^{-5}, λ_1 is 10^{-3}, λ_2 is 10^{-3}, and dropout is 0.6. Finally, for the Citeseer dataset, the learning rate is 10^{-2}, the weight decay is 5×10^{-4}, λ_1 is 10^{-5}, λ_2 is 10^{-5}, and the dropout is 0.6.

We use DeeperGCN models for the OGBN-ArXiv and OGBN-Products datasets. In the case of OGBN-ArXiv, we use a 28-layer DeeperGCN model; for OGBN-Products, we use a 14-layer DeeperGCN model. For OGBN-ArXiv, the learning rate is 10^{-2}, λ_1 is 10^{-6}, and λ_2 is 10^{-6}. For OGBN-Products, the learning rate is 10^{-3}, λ_1 is 10^{-4}, and λ_2 is 10^{-6}. Droput is 0.5 for both the datasets. In the case of heterophilic graphs, we use GPRGNN as the backbone GNN. For the Chameleon dataset, the learning rate is 5×10^{-2}, λ_1 is 10^{-3}, λ_2 is 10^{-3}, and dropout is 0.4. For the Squirrel dataset, the learning rate is 5×10^{-2}, λ_1 is 10^{-6}, λ_2 is 10^{-2}, and dropout is 0.4.

Table 5: Details on the datasets.

Datasets	Type	#Nodes	#Edges	Classes	Features
Cora	Homophilic	2485	5069	7	1433
Citeseer	Homophilic	2110	3668	6	3703
PubMed	Homophilic	19717	44338	3	500
OGBN-ArXiv	Homophilic	169,343	1,166,243	40	128
OGBN-Products	Homophilic	2,449,029	61,859,140	47	100
Chameleon	Heterophilic	2277	62792	5	2325
Squirrel	Heterophilic	5201	396846	5	2089

A.3 Performance Evaluation of ARGS

We evaluate the performance of ARGS on homophilic graphs perturbed by the PGD attack and MetaAttack. We show the results for a 5%, 10%, and 15% perturbation rate for the Cora and Citeseer datasets in Figures 9, 10. Figures 11,and 12 show the performance of ARGS on the Cora and Citeseer datasets with GIN as the backbone GNN. Finally, Figure 13 shows the performance of ARGS on Citeseer with GAT as the backbone GNN. Furthermore, we evaluate the performance of ARGS on the PubMed dataset, as shown in Figure 14.

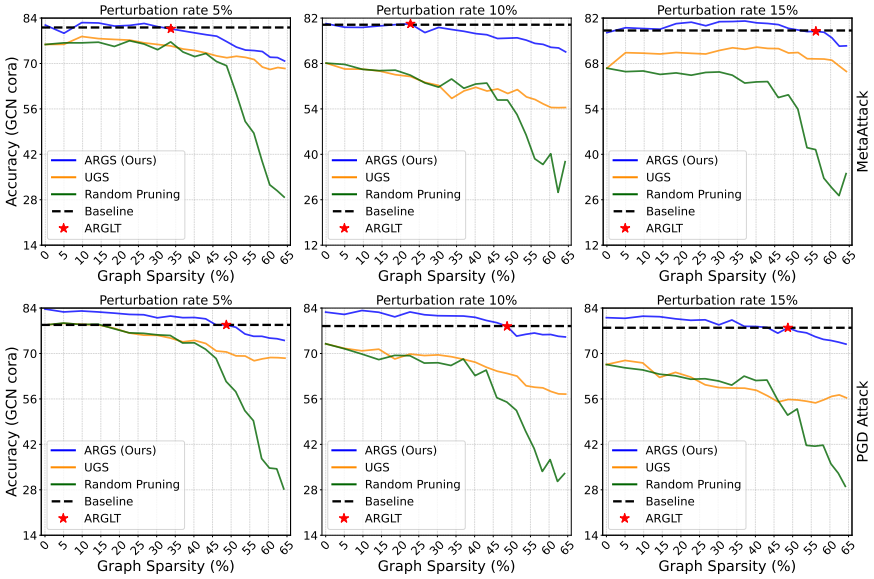

Figure 9: Node classification performance over achieved graph sparsity levels for GCN on the Cora dataset attacked by the PGD attack and MetaAttack. The perturbation rates are 5%, 10%, and 15%. Red stars ⋆ indicate the ARGLTs which achieve similar performance with high sparsity. STRG is used as the baseline.

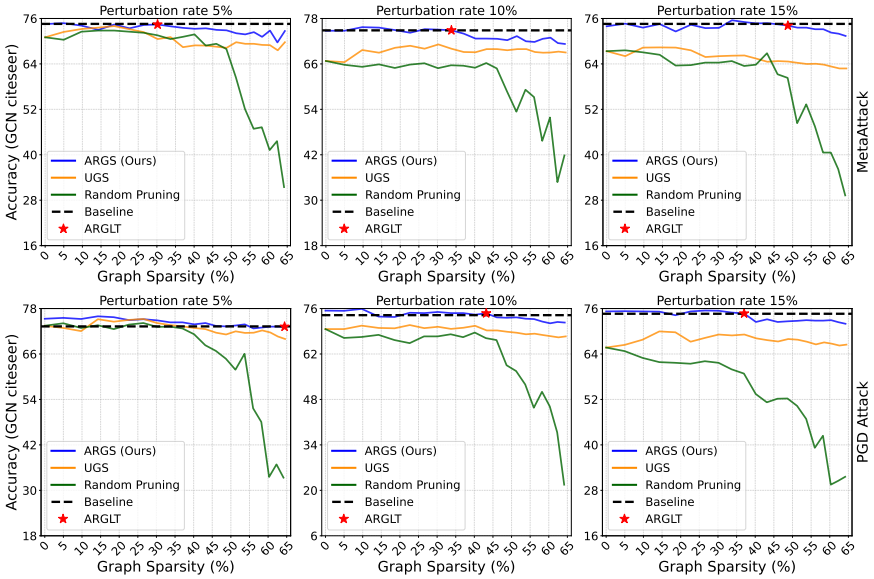

Figure 10: Node classification performance over achieved graph sparsity levels for GCN on the Citeseer dataset attacked by the PGD attack and MetaAttack. The perturbation rates are 5%, 10%, and 15%. Red stars ⋆ indicate the ARGLTs which achieve similar performance with high sparsity. STRG is used as the baseline.

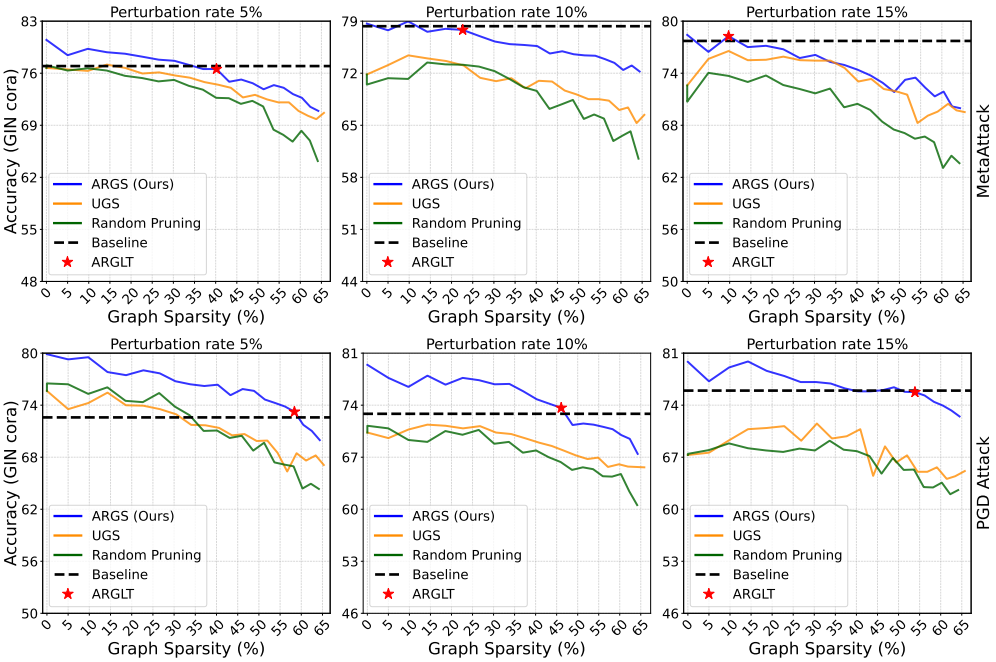

Figure 11: Node classification performance over achieved graph sparsity levels for GIN on the Cora dataset attacked by the PGD attack and MetaAttack. The perturbation rates are 5%, 10%, and 15%. Red stars ⋆ indicate the ARGLTs which achieve similar performance with high sparsity. STRG is used as the baseline.

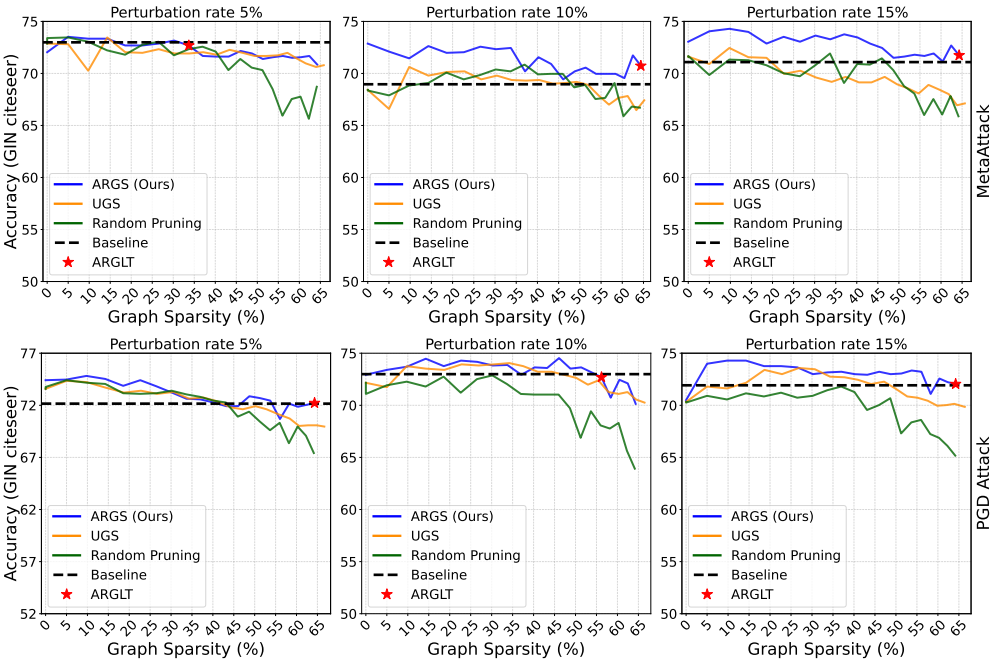

Figure 12: Node classification performance over achieved graph sparsity levels for GIN on the Citeseer dataset attacked by the PGD attack and MetaAttack. The perturbation rates are 5%, 10%, and 15%. Red stars ⋆ indicate the ARGLTs which achieve similar performance with high sparsity. STRG is used as the baseline.

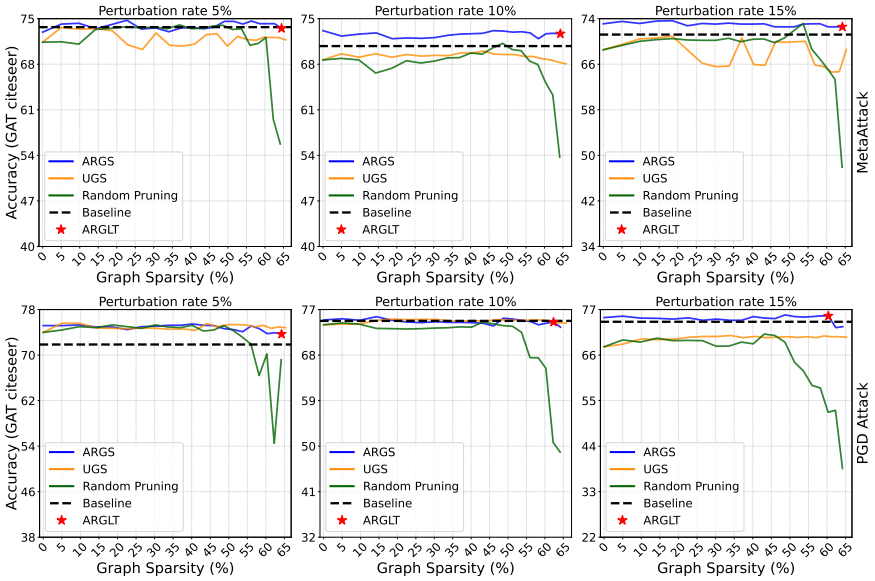

Figure 13: Node classification performance over achieved graph sparsity levels for GAT on the Citeseer dataset attacked by the PGD attack and MetaAttack. The perturbation rates are 5%, 10%, and 15%. Red stars ⋆ indicate the ARGLTs which achieve similar performance with high sparsity. STRG is used as the baseline.

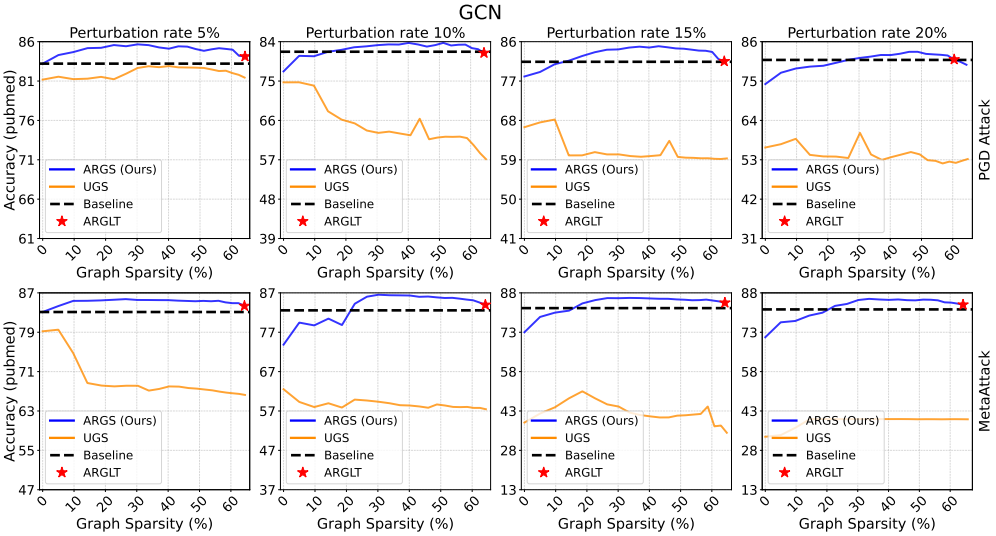

Figure 14: Node classification performance over achieved graph sparsity levels for GCN on the PubMed dataset attacked by the PGD attack and MetaAttack. The perturbation rates are 5%, 10%, 15%, and 20%. Red stars ⋆ indicate the ARGLTs which achieve similar performance with high sparsity. STRG is used as the baseline.

A.4 Comparing the Impact of Node Attribute Features and Positional Features on ARGLTs for Homophilic Graphs

For homophilic graphs, we considered node attribute features for removing the adversarial edges, while node positional features were considered for heterophilic graphs. We then perform a set of experiments, where we instead consider positional features of the nodes for homophilic graphs. We observe that the overlap between the density distribution of positional feature differences of clean edges and that of adversarial edges is higher compared to that of the attribute features. However, the two density distributions of positional feature differences are still separable. The results are reported in Table 6. When positional features are

Table 6: ARGS performance comparison when positional and attribute features are considered for homophilic graphs in the Cora and Citeseer datasets on three different GNN models.

				GCN		GIN		GAT	
Dataset	Attack	Perturbation rate	Feature Type	Graph Sparsity	Model Sparsity	Graph Sparsity	Model Sparsity	Graph Sparsity	Model Sparsity
Cora	PGD	5%	Attribute	**49.2%**	**94.8%**	**58.3%**	**97.2%**	**64.2%**	**98.9%**
			Positional	46.0%	93.3%	**58.3%**	**97.2%**	**64.2%**	**98.9%**
		10%	Attribute	**48.3%**	**94.2%**	**46.0%**	**93.5%**	**64.3%**	**98.9%**
			Positional	37.2%	87.1%	40.1%	89.8%	**64.3%**	**98.9%**
		15%	Attribute	**49.1%**	**94.8%**	**53.7%**	**96.7%**	**64.2%**	**98.9%**
			Positional	37.2%	87.1%	18.5%	59.2%	**64.3%**	**98.9%**
Citeseer	Mettack	5%	Attribute	**31.2%**	**79.4%**	**33.6%**	**83.6%**	**64.2%**	**98.9%**
			Positional	25.8%	74.2%	26.5%	74.2%	**64.2%**	**98.9%**
		10%	Attribute	**33.6%**	**83.6%**	**64.2%**	**98.8%**	**64.2%**	**98.8%**
			Positional	**33.6%**	**83.6%**	**64.2%**	**98.8%**	**64.2%**	**98.8%**
		15%	Attribute	**48.7%**	**94.8%**	**64.2%**	**98.8%**	**64.3%**	**98.8%**
			Positional	43.1%	91.9%	**64.2%**	**98.8%**	**64.3%**	**98.8%**

considered, ARGS is still able to find highly sparse GLTs, but the sparsity levels of the GLTs in some cases are lower than those obtained when attribute features are considered.

A.5 Ablation Study

We perform an ablation study to verify the effectiveness of each component of the proposed loss function used for the sparsification algorithm. Part of this study is already included in the main sections of the paper. We report the rest of the results in Table 7. In particular, we present the analysis performed on the Cora dataset for all the 3 different attacks with all the 4 perturbation rates. We recall that configuration 1 corresponds to ARGS with all the loss components. As shown in Table 7, at both high and low target sparsity, we yield the best classification performance with configuration 1, showcasing the importance of the unified loss function.

Table 7: Ablation study.

GCN, Cora, PGD Attack						Classification Accuracy at Perturbation Rate 5%		Classification Accuracy at Perturbation Rate 15%	
Configuration	α	β	γ	η	ζ	Graph Sparsity 22.7% Model Sparsity 67.7%	Graph Sparsity 60.4% Model Sparsity 98.2%	Graph Sparsity 22.7% Model Sparsity 67.7%	Graph Sparsity 60.4% Model Sparsity 98.2%
1	✓	✓	✓	✓	✓	**82.04**	**74.75**	**80.23**	**73.99**
2	✓	✗	✓	✓	✓	81.84	73.64	79.98	68.81
3	✓	✓	✗	✓	✓	81.69	74.45	76.86	72.89
4	✓	✗	✗	✓	✓	79.28	71.33	74.70	63.48

GCN, Cora, Mettack Attack						Classification Accuracy at Perturbation Rate 5%		Classification Accuracy at Perturbation Rate 10%	
Configuration	α	β	γ	η	ζ	Graph Sparsity 22.7% Model Sparsity 67.6%	Graph Sparsity 62.3% Model Sparsity 98.6%	Graph Sparsity 22.6% Model Sparsity 67.5%	Graph Sparsity 64.2% Model Sparsity 98.9%
1	✓	✓	✓	✓	✓	**81.74**	**71.83**	**80.23**	**71.58**
2	✓	✗	✓	✓	✓	80.89	69.91	78.17	70.98
3	✓	✓	✗	✓	✓	79.88	71.33	75.40	66.81
4	✓	✗	✗	✓	✓	78.89	69.03	75.40	60.97

GCN, Cora, Mettack Attack						Classification Accuracy at Perturbation Rate 15%		Classification Accuracy at Perturbation Rate 20%	
Configuration	α	β	γ	η	ζ	Graph Sparsity 22.7% Model Sparsity 67.6%	Graph Sparsity 60.4% Model Sparsity 98.2%	Graph Sparsity 22.6% Model Sparsity 67.5%	Graph Sparsity 60.3% Model Sparsity 98.2%
1	✓	✓	✓	✓	✓	**80.73**	**75.91**	**79.38**	**70.37**
2	✓	✗	✓	✓	✓	80.23	73.69	78.72	69.97
3	✓	✓	✗	✓	✓	77.97	72.74	75.50	69.16
4	✓	✗	✗	✓	✓	78.42	72.08	74.09	68.86